ACS APPLIED MATERIALS & INTERFACES

Research Article

www.acsami.org

Highly Efficient TiO_2-Based Microreactor for Photocatalytic Applications

Matic Krivec,*[,±,¶] Kristina Žagar,[±] Luka Suhadolnik,[±] Miran Čeh,[±,¶] and Goran Dražić[±,¶,Π]

[±]Department for Nanostructured Materials, Jožef Stefan Institute, Jamova 39, SI-1000 Ljubljana, Slovenia

[¶]Jožef Stefan International Postgraduate School, Jamova 39, SI-1000 Ljubljana, Slovenia

[Π]Department for Materials Chemistry, National Institute of Chemistry, Hajdrihova 19, SI-1000 Ljubljana, Slovenia

ABSTRACT: A photocatalytic, TiO_2-based microreactor is designed and fabricated on a metal−titanium foil. The microchannel is mechanically engraved in the substrate foil, and a double-layered TiO_2 anatase film is immobilized on its inner walls with a two-step synthesis, which included anodization and a hydrothermal treatment. X-ray diffraction (XRD) and scanning electron microscopy (SEM) confirm the presence of an approximately 10-μm-thick layer of titania nanotubes and anatase nanoparticles. The SEM and transmission electron microscopy (TEM) of the cross sections show a dense interface between the titanium substrate and the TiO_2 nanotubes. An additional layer of TiO_2-anatase nanoparticles on the top of the film provides a large, photocatalytic surface area. The metal−titanium substrate with a functionalized serpentine channel is sealed with UV-transparent Plexiglas, and four 0.8-mW UV LEDs combined with a power controller on a small printed-circuit board are fixed over the substrate. The photocatalytic activity and the kinetic properties for the degradation of caffeine are provided, and the longer-term stability of the TiO_2 film is evaluated. The results show that after 6 months of use and 3600 working cycles the microreactor still exhibits 60% of its initial efficiency.

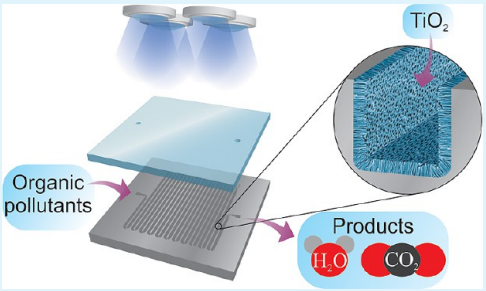

KEYWORDS: *microreactor, anodization, hydrothermal synthesis, TiO_2, photocatalysis*

INTRODUCTION

The remediation of polluted groundwater, toxic industrial wastes, and hazardous chemical substances has attracted attention in many parts of the world. Photocatalytic oxidation with a TiO_2 photocatalyst is considered to be a suitable choice for the relatively cheap and efficient elimination of these chemicals from a variety of media.[1] Furthermore, photocatalysis with TiO_2 can be successfully applied as an efficient route for the selective synthesis of a number of organic molecules, used in the food, pharmaceutical, and cosmetic industries.[2] Most research in photocatalysis for water treatment and selective photocatalytic synthesis in liquid media involves a TiO_2 catalyst in the form of dispersed powders. The slurry reactors with suspended TiO_2 particles have a uniform catalyst distribution and a high photocatalytic surface-to-volume ratio.[3] For any practical use, however, this is not the preferred configuration. The TiO_2 particles have to be additionally separated from the products and recycled, which is an expensive and time-consuming process. In most cases it is also impossible to completely remove all the titania nanoparticles from the liquid. Furthermore, the penetration depth of the UV light is rapidly decreasing due to the strong absorbing properties of the suspended TiO_2 particles and other organic molecules. Immobilized photocatalysts are therefore a better and more practical option for photocatalytic reactions. The main drawback of photocatalysis in the presence of immobilized TiO_2 is the limited amount of exposed TiO_2 surface area, which in most cases leads to mass-transfer limitations.[4]

The design of a highly effective photoreactor is crucial in order to get the highest possible reaction rates with the immobilized form of TiO_2. In recent years, microreactor technology has become a valuable tool for the chemical industry and mobile applications of chemical systems. A laminar flow, short molecular diffusion distances, large surface-to-volume ratios, a high spatial illumination homogeneity, and good light penetration through the entire reactor depth are some of the many characteristics that give processes inside microreactors an advantage over those in conventional reactors.[5,6] Photocatalytic microreactors with an immobilized TiO_2 catalyst have already proven to be a highly effective tool for the degradation and synthesis of different organic molecules and for the selective cleavage of peptides and proteins, which can be very beneficial for the synthesis of fine chemicals, pharmaceutical industries, and proteomics laboratories.[7−9] Moreover, photocatalytic microreactors can be optimized for a particular function in a research laboratory, because they do not have to undergo a scaling-up process. Using several microreactors in parallel ('numbering up') provides the possibility for the continuous industrial production of photocatalyzed products.[8]

There have already been reports of microstructured reactors with immobilized TiO_2 on their inner walls. Choi et al. applied

Received: June 20, 2013
Accepted: August 26, 2013
Published: August 26, 2013

a TiO_2 coating on the walls of capillary microtubes using a wash-coating technique with an aged titania gel and a subsequent calcination.[10] A similar technique was used in the work of Rebrov et al., where they report on the synthesis of an approximately 120-nm-thick TiO_2 film inside a silica capillary.[11] The group of Lindstrom deposited a 1-μm-thick titania film inside a soda-lime glass microchannel using a continuous flow of a colloidal TiO_2 suspension through the microreactor.[12] On the other hand, Matsushita et al. functionalized an unmounted reactor with a spin-coating of titanium tetra-isopropoxide solution on a glass and Pyrex substrate with an inscribed microchannel, which was additionally covered with a window plate and sealed.[13] The interface between the TiO_2 film and the substrate, the stability (aging), and the reproducibility of the photocatalytic microreactors were not investigated. The electrochemical oxidation of the titanium substrate has also been applied as a TiO_2-immobilization technique. The authors reported that the contact between the TiO_2 film and the substrate (titanium) improved and the surface area of the nanostructures increased.[14,15] The electrochemical oxidation (anodization) of the titanium foil produces perfectly self-aligned, TiO_2 nanotube assemblies that possess a high aspect ratio and are frequently used as efficient photoanodes in dye-sensitized solar cells (DSSCs).[14−16] In the past five years there has been an increased interest in the research on TiO_2, aligned nanotube arrays formed by anodization due to their interesting and unique combination of geometry and their chemical and physical functionalities.[16] Furthermore, the geometry (wall thickness, length, diameter, and the intertube spacing) of the TiO_2 nanotube arrays can be easily tailored by controlling the processing parameters, such as the time of the anodization, the type and pH of the electrolyte, the temperature, the applied potential, etc.[15] Anodization has the advantage of a selective and homogeneous functionalization of different shapes of titanium substrates, e.g., microchannels, with titania nanotubes. Moreover, well-bounded titania structures can be subsequently treated with different techniques, and their surface can be enhanced with additional titania particles in order to improve the adsorption of pollutants and other molecules that participate in the photocatalytic reaction.

In the present paper we report on the fabrication and properties of a titanium photomicroreactor with an immobilized TiO_2 photocatalyst and an integrated UV-LED source. A novel, two-step synthesis (anodization and a subsequent hydrothermal treatment) was applied for the preparation of a double-layered, anatase, TiO_2 film. This method provides a homogeneous distribution of a strongly bound and photocatalytically active TiO_2 coating on the inner surface of the microchannel. The kinetic parameters, efficiencies, and stability of the reactor were evaluated with the oxidation of a caffeine molecule, followed by UV−vis spectroscopy.

EXPERIMENTAL SECTION

Materials. Titanium foil (99.6%, dimensions: 25 × 25 × 1 mm, annealed, Goodfellow Cambridge Limited, Huntington, England), polymethyl-methacrylate sheet (Plexiglas, UV transparent, dimensions: 25 × 25 × 2 mm, Acrytech d.o.o., Ljubljana, Slovenia), fluorinated ethylene propylene tubing (internal diameter: 0.5 mm, Vici AG International, Schenkon, Switzerland), titanium(IV) chloride ($TiCl_4$, 99.9%, Acros Organics, New Jersey, USA), ethylene glycol (99.5%, Carlo Erba Reagents, Val de Reuil, France), ammonium fluoride (Kemika d.d., Zagreb, Croatia), and caffeine (≥99.0% HPLC grade, Sigma-Aldrich Chemie GmbH, Steinheim, Germany) were used without further purification.

Microreactor Fabrication. The microreactor device was fabricated from a titanium foil in which a serpentine microchannel with cross-section dimensions of approximately 500 μm × 500 μm and a length of 390 mm was engraved using a high-precision CNC milling machine. The substrate was then rinsed with absolute ethanol in an ultrasonic bath for several minutes. Afterward, the titanium surface with the microchannel inner walls was coated with a mixture of TiO_2 nanotubes and nanoparticles in a two-step synthesis, which included anodic oxidation and a hydrothermal treatment. The detailed synthesis will be explained in the next paragraph. After the synthesis, the TiO_2 film inside the microchannel was protected with high-purity wax, and the upper surface of the microreactor was ground and polished in order to prepare a smooth titanium surface for the next step of the microreactor fabrication, i.e., sealing. UV-transparent Plexiglas with the same dimensions as the titanium foil and with two holes of 2 mm in diameter (inlet and outlet) was put on the top of the microchannel and sealed with epoxy glue. Plastic inert tubing was used for connecting the inlet of the reactor with a high-precision syringe pump (Aladdin, World Precision Instruments, Sarasota, USA) and the outlet with the tubes for sample collection. The whole device was afterward mounted in a stainless-steel housing. Four 0.8-mW UV-LED diodes (Roithner Lasertechnik GmbH, Vienna, Austria) with an emission maximum at 365 nm were mounted on a circuit board with an integrated power controller and placed on the top of the microreactor housing. The incident light intensity of 1.2 mW cm^{-2} was measured at a distance of 3 mm.

Synthesis of TiO_2 Film. The TiO_2 film was prepared with a two-step synthesis. In the first step, titania nanotube arrays were produced by an anodization process using commercially available titanium foil. The titania nanotubes were synthesized according to the procedure reported by Shankar et al.[14] In brief, the titanium foil was first rinsed with acetone and ethanol in an ultrasonic bath to remove any organic impurities. After cleaning, the anodization was performed at room temperature in a two-electrode electrochemical cell connected to a dc power supply of 60 V for 3 h, while the anodization current and electrolyte temperature were monitored. The electrolyte used was an ethylene glycol solution with a small portion of NH_4F (0.3 wt %) and H_2O (2 vol%). In the second step (hydrothermal synthesis) the anodized microreactor was positioned on the bottom of a Teflon-lined stainless-steel autoclave that was filled with a water suspension of $TiCl_4$ (0.2 M, 50% filling). The autoclave was placed inside an oven (Binder FED 53) that was set to 75 °C for 1 h. The as-prepared microreactor was washed with absolute ethanol for several times and calcinated at 400 °C for 3 h (heating rate was 5 °C/min). The TiO_2 film was characterized with X-ray diffraction (XRD, PANalytical X'Pert PRO diffractometer), a focused-ion-beam workstation (FIB, FEI Helios Nanolab650), and a transmission electron microscope (TEM, JEOL 2010F). The TEM cross-section specimen was prepared with conventional ion-milling (Gatan, Model 691 PIPS).

Photocatalytic Experiments. The photocatalytic efficiency of the photomicroreactor was investigated by measuring the degradation of caffeine. Caffeine was chosen as a model degradation molecule for various reasons, i.e., it is the origin of domestic sanitary contamination and the mechanism of its degradation has already been investigated in an aqueous suspension of TiO_2 particles.[17−19] Four different initial concentrations (25, 10, 5, 2.5 mg L^{-1}) were examined, and a high-precision UV−vis-IR spectrometer (PerkinElmer Lambda 950) was used for the characterization of the caffeine concentration for six different volumetric flow rates (100, 80, 60, 40, 30, 20 μL min^{-1}) operating under continuous flow. The caffeine solution (200 μL) was continuously pumped through the microreactor before each measurement in order to clean the reactor. A dark sample (without illumination) was collected at each flow rate to get an insight into the caffeine adsorption on the TiO_2 film. The degradation of each initial caffeine concentration was repeated two times, and the average value is presented in the results. The kinetic measurements and photonic efficiencies were determined from the initial degradation rates (R_i), calculated from the initial slopes of the caffeine degradation at a certain initial concentration.

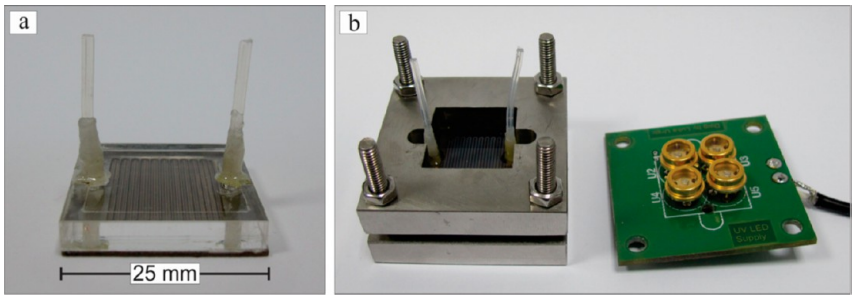

Figure 1. TiO_2-based microreactor: a) without housing and b) with housing and UV-LED supply.

RESULTS AND DISCUSSION

Microreactor Design. Figure 1 shows the serpentine-shaped microreactor. The characteristics of the microreactor are summarized in Table 1. A 390-mm-long and 0.5-mm-wide microchannel was mechanically engraved in the metal−titanium foil. The grinding and polishing of the reactor surface after the TiO_2 synthesis resulted in a reduction of the channel depth to 0.36 mm. A high surface-to-volume ratio is one of the essential advantages of microreactors. In this case the calculated value (6780 m^2 m^{-3}) is comparable with the values reported by Van Gerven et al.[20] The UV-LED intensity with a maximum at 365 nm was measured with a UV-A meter (Dr. Hönle AG, Germany) at different distances from the reactor surface, and an optimal position (3 mm) was determined, taking account of the emission pattern and the angle of the light source. The temperature stability of the reactor, measured with a thermocouple, showed a negligible increase in the temperature (1.5 °C) after longer irradiation times (5 h) and confirmed a good heat exchange inside the reactor, without the necessity for an additional cooling system.

Table 1. Characteristics of TiO_2-Based Microreactor

microreactor	value
channel length (mm)	390
channel depth (mm)	0.36
channel width (mm)	0.5
reactor volume (μL)	70
surface area (mm^2)	476[a]
surface-to-volume ratio (m^2 m^{-3})	6780[a]
UV-LED intensity (mW cm^{-2})	1.2[b]
temperature stability (K h^{-1})	0.3

[a]Values were calculated without taking into account the specific surface area of the TiO_2 film. [b]The total integrated incident intensity between 330 and 400 nm from four UV-LED diodes.

The TiO_2 photocatalyst was immobilized on the inner walls of the microchannel in a two-step synthesis (Figure 2). In the first step the TiO_2 nanotubes were synthesized on the top of a titanium substrate with anodic oxidation. This process provides a homogeneous distribution of titania nanotubes, and the diameter of the tubes and their length can be adjusted by changing the experimental conditions. In the second step, additional TiO_2 nanoparticles were produced and deposited on the top of the nanotube arrays with a hydrothermal synthesis in order to increase the TiO_2 surface area and improve the overall photocatalytic efficiency of the microreactor. The functionalized inner walls of the microchannel were protected with high-purity wax, and the titania film on the other surfaces of the metal foil was removed by grinding and polishing. The microchannel was covered with UV-transparent Plexiglas and placed in a stainless-steel housing.

Characterization of TiO_2 Film. The X-ray diffraction pattern in Figure 3 shows the presence of a single-anatase-phase TiO_2 film. The additional peaks correspond to the titanium substrate.

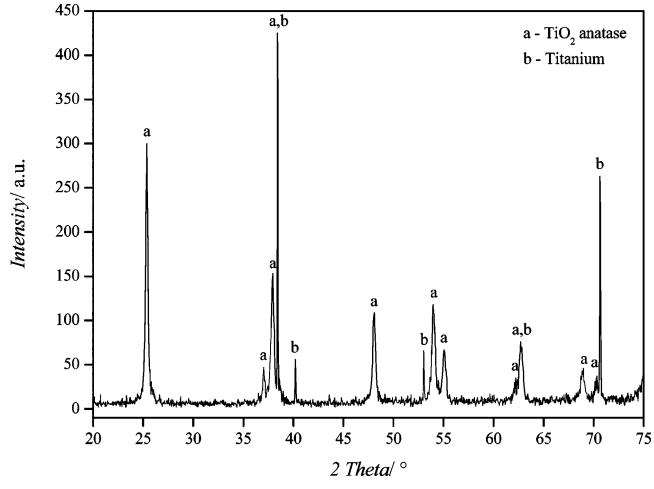

Figure 3. XRD pattern of TiO_2 film synthesized with a combination of the anodic oxidation of titanium and a hydrothermal treatment after annealing at 400 °C for 3 h.

The microstructure and the composition of an approximately 10-μm-thick TiO_2 film were characterized with SEM and a

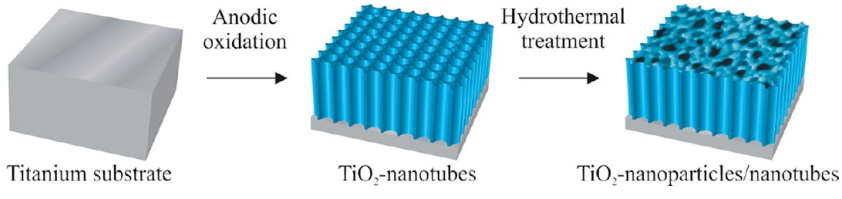

Figure 2. 3D schematic picture of the two-step synthesis: anodic oxidation of titanium substrate and subsequent hydrothermal treatment.

focused ion beam (FIB). The top-view SEM picture (Figure 4) reveals the surface morphology of the TiO_2 film, which

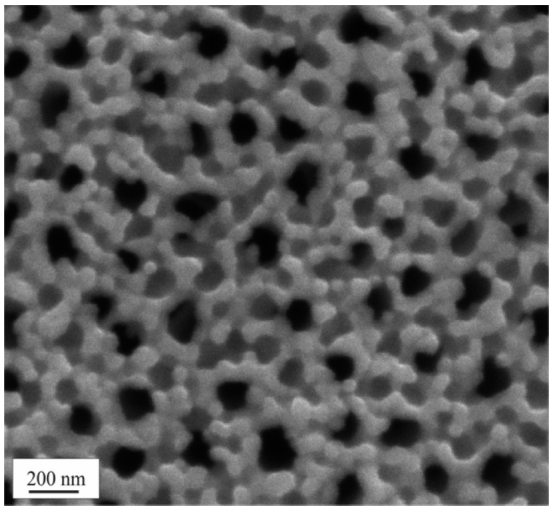

Figure 4. SEM micrograph of TiO_2 nanoparticle/nanotube dual-layer from a top view.

consisted of titania nanotubes with a hole diameter of around 100 nm that are covered with a thin layer of small titania nanoparticles. This surface layer was synthesized during the hydrothermal treatment, where the combination of etching the amorphous TiO_2 nanotubes with HCl (side product of $TiCl_4$ hydrolysis) and the synthesis of TiO_2 nanoparticles resulted in a titania surface with a high overall surface area.

The cross sections in Figure 5 were prepared by FIB milling of the TiO_2 film perpendicular to the titanium substrate. A thin layer of platinum was deposited on the top of the TiO_2 film in order to prevent the deformation of the surface with high-energy gallium ions (Figure 5a). A higher-magnification SEM image (inset of Figure 5a) shows the two-phase cross-section, where a 100-nm-thick surface layer consisting of TiO_2 nanoparticles uniformly covers the titania nanotubes. The interface between the titania nanotubes and the titanium substrate is shown in Figure 5b. To avoid the curtains effect, where the topography of the nanotubes would continue into the titanium substrate, the cross-sectional cut of the metal/nanotubes interface was performed from the metal titanium side.[21] The inset of Figure 5b shows a stable contact between the phases. The upper, darker part of the micrograph shows longitudinal cuts of the TiO_2 nanotubes with several defects (from the sample preparation), while the lower, brighter titanium part has a smooth, homogeneous structure without visible imperfections.

The TEM micrograph (Figure 6) shows the interface between the titanium support and the titania nanotube film. The phase composition was determined with selected-area electron diffraction (SAED) patterns (Figure 6a) for different regions of the cross-section: the lower part of the cross-section is composed only of titanium grains, without any oxidized inclusions; while the scaffold and the body of the nanotubes are built from pure anatase-phase crystals. Additional diffraction spots for the rutile phase were found at the TiO_2/titanium interface (inset of Figure 6b). This agrees with the results of Varghese et al., where they claimed that the phase transformation from anatase to rutile at relatively low annealing temperatures (400 °C) occurs only at the nanotube/titanium

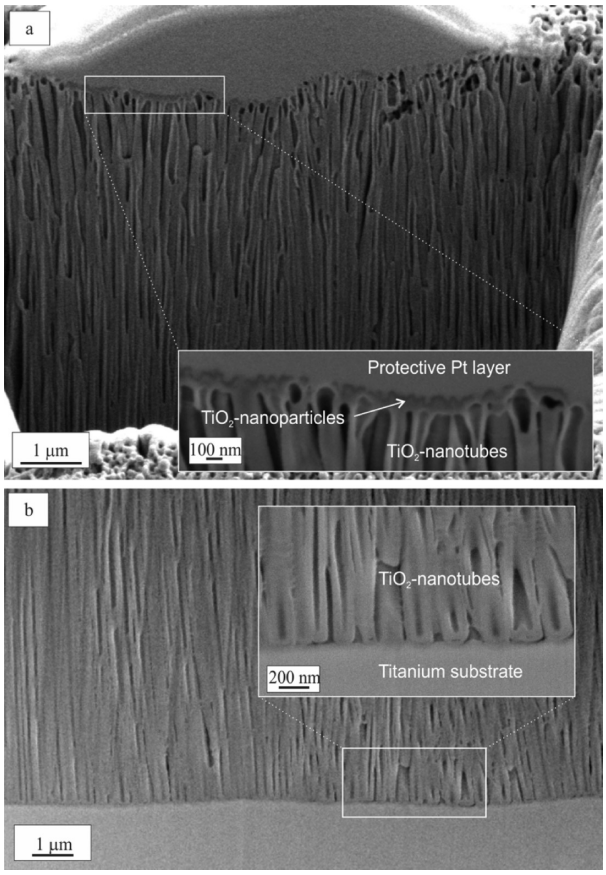

Figure 5. SEM micrographs of the cross-section of the TiO_2 nanoparticle/nanotube dual-layer: a) nanoparticle/nanotube interface and b) nanotube/titanium substrate interface.

support interface.[22] The micrograph of the interface at higher magnification shows that a dense boundary without visible defects, voids, or cracks was preserved between the oxidized barrier layer and the titanium support during the TEM sample preparation (micromilling and ion slicing). This confirms the good mechanical properties of the titania film that was synthesized with the anodization procedure.

Photocatalytic Activity. The photocatalytic degradation of the caffeine starts with the breaking of the C4═C5 double bond due to the reaction with hydroxyl radicals, which results in the formation of dimethylparabanic acid. The second degradation intermediate, di(N-hidroxymethyl)parabanic acid, is formed as a product of the oxidation of N-methyl groups, which then proceeds with a final mineralization to CO_2, NH_3, and NH_2Me.[23] While the formation of these two intermediates is rather fast, the complete mineralization is much slower, and, therefore, the short reaction times of our experimental setup with the microreactor are not suitable for complete mineralization and, consequently, TOC (total organic carbon) measurements were not performed. However, the reduction of the characteristic UV band of caffeine at 274 nm gave us an insight into the caffeine degradation with the photomicroreactor and the possibility to determine its activity, stability and kinetic properties.

The photodegradation of the caffeine was investigated with the use of an aged microreactor. Several organic molecules (dichloroacetic acid, terephthalic acid, and formic acid) were intensively tested for 6 months as potential model pollutants for the photocatalytic characterization of the microreactor (to

dx.doi.org/10.1021/am402389t | ACS Appl. Mater. Interfaces 2013, 5, 9088−9094

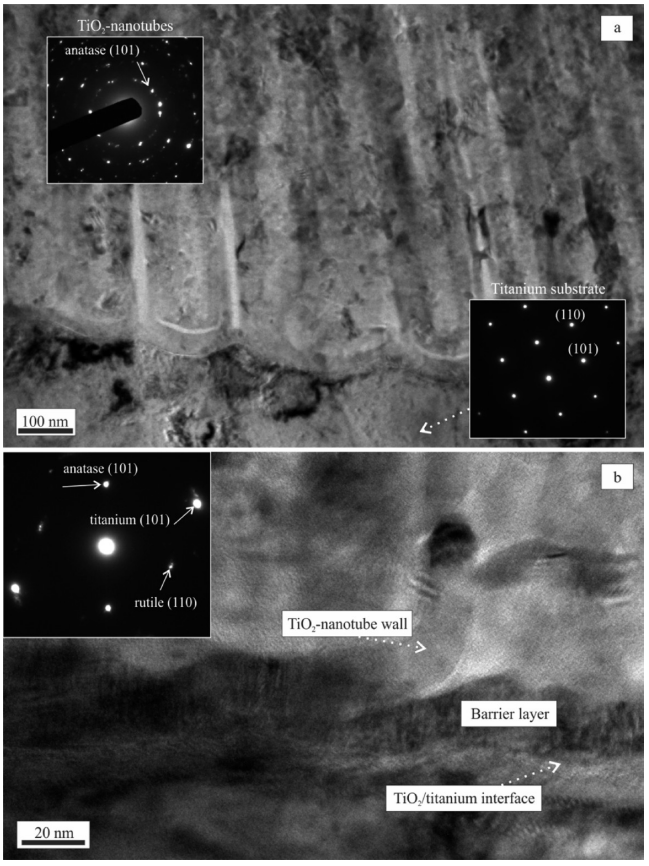

Figure 6. TEM micrographs of the TiO_2 nanotube/titanium support cross-section: a) SAED patterns at different regions of the sample and b) nanotube/titanium interface at higher magnification.

be published). The results of the photodegradation of caffeine at different hydrodynamic residence times, calculated from the equation $\tau = V/q_v$, where V is the reactor volume and q_v is volumetric flow rate, are shown in Figure 7a. A higher degradation was observed at lower initial concentrations of caffeine. Furthermore, the degradations with the lowest caffeine concentrations (2.5 and 5 mg L^{-1}) are almost identical. This behavior can be explained by the function of the diffusion, which is a critical factor in the continuous degradation of smaller quantities of pollutant, while the molecules cannot get into contact with the photocatalyst in time to initiate the reaction. The effect of the initial caffeine concentration on the reaction rate (R_i) is shown in Figure 7b. The initial reaction rates increase with the increasing initial caffeine concentration and come to a plateau at around 0.06 mM. This suggests that the rate of degradation is limited by the adsorption of the caffeine molecules on the photocatalyst, which follows the Langmuir–Hinshelwood (L–H) equation[24]

$$R_i = -\frac{d[\text{caffeine}]}{dt} = \frac{k_a K c_i}{1 + K c_i}$$

where k_a is the apparent reaction-rate constant, K is the adsorption coefficient, and c_i is the initial concentration of caffeine. The linearization of the Langmuir–Hinshelwood equation results in a linear relationship with an intercept of k_a^{-1} and a slope of $(k_a K)^{-1}$:

$$\frac{1}{R_i} = \frac{1}{k_a} + \frac{1}{k_a K}\frac{1}{c_i}$$

The reaction-rate constant (k_a) of 1.82 mmol L^{-1} h^{-1} and the adsorption coefficient (K) of 17 L $mmol^{-1}$ were derived from the intercept and slope of the linear line shown in the inset of Figure 7b. For comparison, the reactions of caffeine degradation were conducted in a 10 mL slurry reactor using a commercial Degussa P25 powder, and the kinetic properties

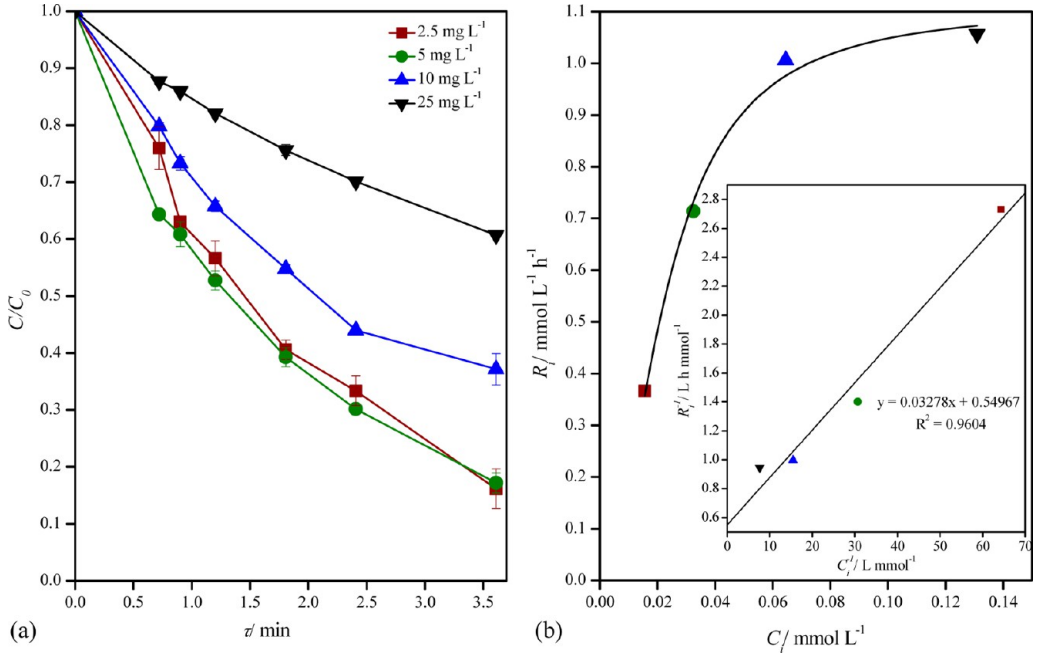

Figure 7. (a) Photocatalytic degradation of caffeine in the photomicroreactor at different hydrodynamic residence times for different initial concentrations and (b) the variation of the initial reaction rate with respect to the initial concentration. The inset diagram shows the linearization of the data.

were evaluated (not shown). While the k_a value varies a great deal with the experimental conditions, the K value determined with the slurry reactor (14 L mmol^{-1}) agrees with the value determined using the microreactor.

Photonic efficiency (ξ) is a well-recognized parameter in photochemistry that enables a comparison of the results between different groups dealing with advanced oxidation processes. It is defined as the number of transformed reactant molecules divided by the number of incident photons of monochromatic light on the front window of the reactor. Alternatively, ξ can be simplified as[25]

$$\xi = \frac{\text{rate of reaction}}{\text{incident monochromatic light intensity}}$$

The photonic efficiencies were calculated from the initial reaction rates (R_i) for different initial concentrations of caffeine and are presented in Table 2.

Table 2. Initial Reaction Rates (R_i) and Photonic Efficiencies (ξ) for Different Initial Concentrations (C_i) of Caffeine

C_i (mg L^{-1})	R_i (mmol L^{-1} h^{-1})	ξ (%)[a]
2.5	0.37	0.103
5	0.71	0.200
10	1.01	0.291
25	1.06	0.378

[a]Values were calculated with the assumption of an equal homogeneous illumination on the bottom of the microchannel.

The values are rather low, which suggests that a large number of incident photons is lost during the reaction or, in other words, only a small portion of them actually participate in the photocatalytic reaction. The highest photonic efficiency (0.378%) was determined with the degradation of the highest initial concentration of caffeine (25 mg L^{-1}). Other groups, dealing with the photocatalytic degradation of caffeine, did not provide the values for photonic efficiencies; therefore, a direct comparison was not possible. However, Gorges et al. reported photonic efficiencies of 0.016−0.026% for the degradation of 4-chlorophenol inside a photocatalytic microreactor.[6] Their values are approximately 10 times lower than ours, although different degradation mechanisms and adsorption properties of the two molecules prevent a direct comparison of the experiments.

The stability of the microreactor was estimated by comparing the photocatalytic activity of the aged reactor with the first photocatalytic degradation experiments involving caffeine, which were conducted with a newly prepared reactor. It is important to point out that in between the experiments the microreactor was extensively studied and used for the degradation of different pollutant molecules. The total volume of the reactor was replaced 3600 times in a longer period of time (6 months), and an estimated volume of 250 mL with an average flow of 40 μL min^{-1} was pumped through the reactor. The photocatalytic activity of the microreactor evidently decreases after a series of experiments, while a decay in the degradation of caffeine was observed (Figure 8). The evaluated initial reaction rate (R_i) of the aged reactor was 40% smaller than the rate of the fresh reactor under the same experimental conditions. This behavior can be explained by several effects. The first one is the washing-out and the elimination of a certain amount of surface TiO_2 nanoparticles (erosion), which

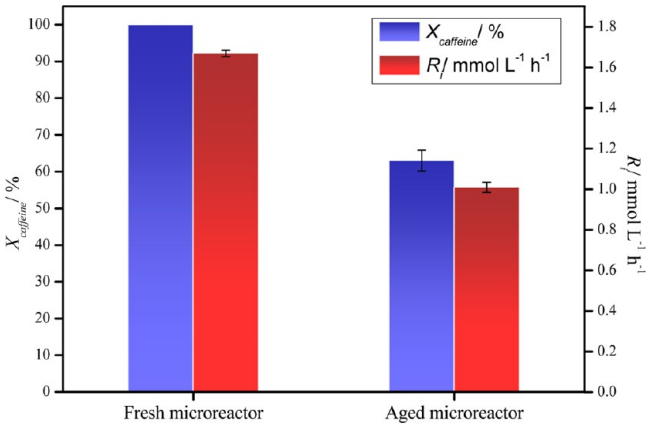

Figure 8. Photocatalytic conversion of caffeine (C_i = 10 mg L^{-1}) after a 3.6-min residence time (τ) and initial reaction rates (R_i) in the freshly synthesized and aged photomicroreactor after 6 months and 3600 cycles.

decreases the catalytic surface area and consequently the adsorption of caffeine molecules on the photocatalyst. The next possible effect is the fouling of the catalyst: the adsorbed byproducts inhibit the adsorption of the pollutant and decrease the potential activity of the catalyst.[26] The third possibility is dissolution of the nanoparticles and the deformation of the surface titania layer in aggressive substances (model pollutants and their byproducts). The washing-out effect was analyzed by determining the TiO_2 nanoparticles' concentration in the product solution using a standardized analytical method for the determination of asbestos fibers in water (EPA Method 100-1).[27] The freshly prepared microreactor was washed with 40 mL of caffeine solution under UV illumination in order to simulate its standard operating conditions. Although this volume represented around 570 cycles of the complete reactor-volume replacement and more than 15% of the whole volume being pumped through the microreactor throughout the study, we did not detect any titania particles in the drained solution. Therefore, we confirmed that there is no short-term erosion of nanoparticles from the microchannel, although we cannot neglect the possibility of the washing-out effect after longer times of use. The negative effect of fouling could be avoided by the regeneration of the catalyst. So the illuminated microreactor was washed with deionized water several times in order to mineralize the adsorbed byproducts and increase the adsorption of caffeine. The activity of the reactor did not improve; therefore, we can conclude that fouling was not the key reason for the decreased activity. The partial nonreversible deactivation of the microreactor is most probably due to the dissolution of the surface titania nanoparticles and their further erosion during long-term operation of the reactor. Nevertheless, the photocatalytic results in Figure 7 and Table 2 still show significant photocatalytic activity after long-term use. Further experiments are being planned to replace the substrate material with the more commercially available aluminum and to improve and prolong the activity of the reactor by increasing the photocatalytic surface area (hydrothermal treatment) and reducing the recombination rate (deposition of platinum or silver nanoparticles).

CONCLUSION

An original, two-step synthesis was used to produce a double-layered TiO_2 film that was immobilized on the inner walls of a

titanium microreactor. The lower part of the titania film in the form of nanotubes, created during anodization, formed a stable interface with the titanium substrate, while the upper part consisting of TiO_2 nanoparticles, prepared during hydrothermal synthesis, increased the catalytic surface of the film and played a major role in the photocatalytic process. The metal substrate with a functionalized serpentine channel was sealed with UV-transparent Plexiglas and integrated with a UV-LED diode source and power supply. A thorough photocatalytic characterization was performed using caffeine as a model pollutant. The photocatalytic degradation of caffeine in a TiO_2-based microreactor follows the Langmuir–Hinshelwood mechanism, and the apparent reaction rate constant (k_a) of 1.82 mmol L^{-1} h^{-1} and the adsorption coefficient (K) of 17 L $mmol^{-1}$ were determined. The microreactor still exhibited 60% of its initial activity after extensive use over an extended period of time (6 months, 3600 cycles). The decrease in the efficiency is most probably due to the dissolution of surface titania nanoparticles and a reshaping of the TiO_2 surface after long-term use of the microreactor.

AUTHOR INFORMATION

Corresponding Author

*E-mail: matic.krivec@ijs.si.

Notes

The authors declare no competing financial interest.

ACKNOWLEDGMENTS

This work was financially supported by the Slovenian Research Agency within the program P2-0084 and project J2-4309. The work is part of the Ph.D. thesis of M. Krivec under Grant no. PR-03769. The assistance of M. Gec, A. Ivekovič, L. Uršič, and J. Zavašnik is gratefully acknowledged.

REFERENCES

(1) Hoffmann, M. R.; Martin, S. T.; Choi, W.; Bahnemann, D. W. *Chem. Rev.* **1995**, *95*, 69–96.

(2) Palmisano, G.; Augugliaro, V.; Pagliaro, M.; Palmisano, L. *Chem. Commun.* **2007**, 3425–3437.

(3) de Lasa, H.; Serrano-Rosales, B.; Salaices-Arredondo, M. In *Photocatalytic Reaction Engineering*; Springer Science+Business Media: New York, 2005; pp 19—21.

(4) Ray, A. K.; Beenackers, A. A. C. M. *AIChE J.* **1998**, *44*, 477–483.

(5) Jänisch, K.; Hessel, V.; Löwe, H.; Baerns, M. *Angew. Chem., Int. Ed.* **2004**, *43*, 406–446.

(6) Gorges, R.; Meyer, S.; Kreisel, G. *J. Photochem. Photobiol., A* **2004**, *167*, 95–99.

(7) Coyle, E. E.; Oelgemöller, M. *Photochem. Photobiol. Sci.* **2008**, *7*, 1313–1322.

(8) Roberge, D. M.; Ducry, L.; Bieler, N.; Cretton, P.; Zimmermann, B. *Chem. Eng. Technol.* **2005**, *28*, 318–323.

(9) Jones, B. J.; Vergne, M. J.; Bunk, D. M.; Locascio, L. E.; Hayes, M. A. *Anal. Chem.* **2007**, *79*, 1327–1332.

(10) Choi, B.-C.; Xu, L.-H.; Kim, H.-T.; Bahnemann, D. W. *J. Ind. Eng. Chem.* **2006**, *5*, 663–672.

(11) Rebrov, E. V.; Berenguer-Garcia, A.; Skelton, H. E.; Johnson, B. F. G.; Wheatley, A. E. H.; Schouten, J. C. *Lab Chip* **2009**, *9*, 503–506.

(12) Lindstrom, H.; Wootton, R.; Iles, A. *AIChE J.* **2007**, *53*, 695–702.

(13) Matsushita, Y.; Ichimura, T.; Ohba, N.; Kumada, S.; Sakeda, K.; Suzuki, T.; Tanibata, H.; Murata, T. *Pure Appl. Chem.* **2007**, *79*, 1959–1968.

(14) Shankar, K.; Mor, G. K.; Prakasam, H. E.; Yoriya, S.; Paulose, M.; Varghese, O. K.; Grimes, C. A. *Nanotechnology* **2007**, *18*, 65707–65718.

(15) Sun, L.; Zhang, S.; Sun, X.; He, X. *J. Nanosci. Nanotechnol.* **2010**, *10*, 4551–4561.

(16) Ghicov, A.; Schmuki, P. *Chem. Commun.* **2009**, *20*, 2791–2808.

(17) Chuang, L.-C.; Luo, C.-H.; Huang, S.-W.; Wu, Y.-C.; Huang, Y.-C. *Adv. Mater. Res.* **2011**, *214*, 97–102.

(18) Sauvé, S.; Aboulfadl, K.; Dorner, S.; Payment, P.; Deschamps, G.; Prévost, M. *Chemosphere* **2012**, *86*, 118–123.

(19) Krivec, M.; Segundo, R. A.; Faria, J. L.; Silva, A. M. T.; Dražić, G. *Appl. Catal., B* **2013**, *140–141*, 9–15.

(20) Van Gerven, T.; Mul, G.; Moulijn, J.; Stankiewicz, A. *Chem. Eng. Process.* **2007**, *46*, 781–789.

(21) Ishitani, T.; Umemura, K.; Ohnishi, T.; Yaguchi, T.; Kamino, T. *J. Electron. Microsc.* **2004**, *53*, 443–449.

(22) Varghese, O. K.; Gong, D.; Paulose, M.; Grimes, C. A.; Dickey, E. C. *J. Mater. Res.* **2003**, *18*, 156–165.

(23) Dalmazio, I.; Santos, L. S.; Lopes, R. P.; Eberlin, M. N.; Augusti, R. *Environ. Sci. Technol.* **2005**, *39*, 5982–5988.

(24) Theurich, J.; Lindner, M.; Bahnemann, D. W. *Langmuir* **1996**, *12*, 6368–6376.

(25) Mills, A.; Le Hunte, S. *J. Photochem. Photobiol., A* **1997**, *108*, 1–35.

(26) Subba Rao, K. V.; Subrahmanyam, M.; Boule, P. *Appl. Catal., B* **2004**, *49*, 239–249.

(27) United States Environmental Agency, Environmental Research Laboratory. *Analytical Method for Determination of Asbestos Fibers in Water*; Athens, USA, 1983.